Electronic Supplementary Information

Bioreducible, arginine-rich polydisulfide-based siRNA nanocomplexes with excellent tumor penetration for efficient gene silencing

Xinyue Zhang, [a,b] Kai Hong,[b] Qingmei Sun,[b] Yunqing Zhu,*[,a,b] and Jianzhong Du*[,a,b]

[a] *Department of Orthopedics, Shanghai Tenth People's Hospital, Tongji University, 301 Middle Yanchang Road, Shanghai 200072, China.*

[b] *Department of Polymeric Materials, School of Materials Science and Engineering, Tongji University, 4800 Caoan Road, Shanghai 201804, China.*

**Corresponding Author. jzdu@tongji.edu.cn (J.D.); 1019zhuyq@tongji.edu.cn (Y.Z.)*

Figures, Tables and Calculations

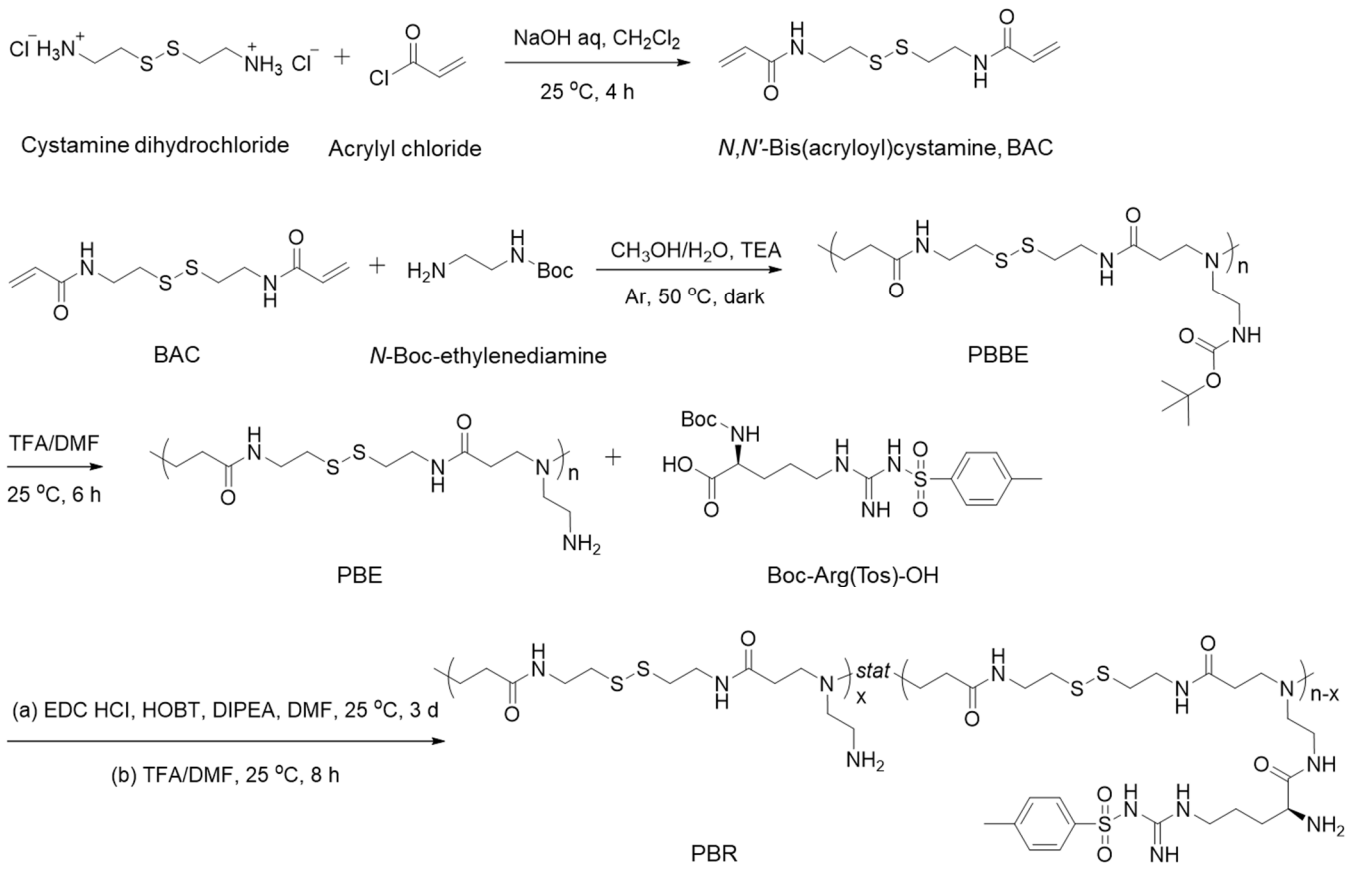

Fig. S1 Syntheses of monomer and polymers.

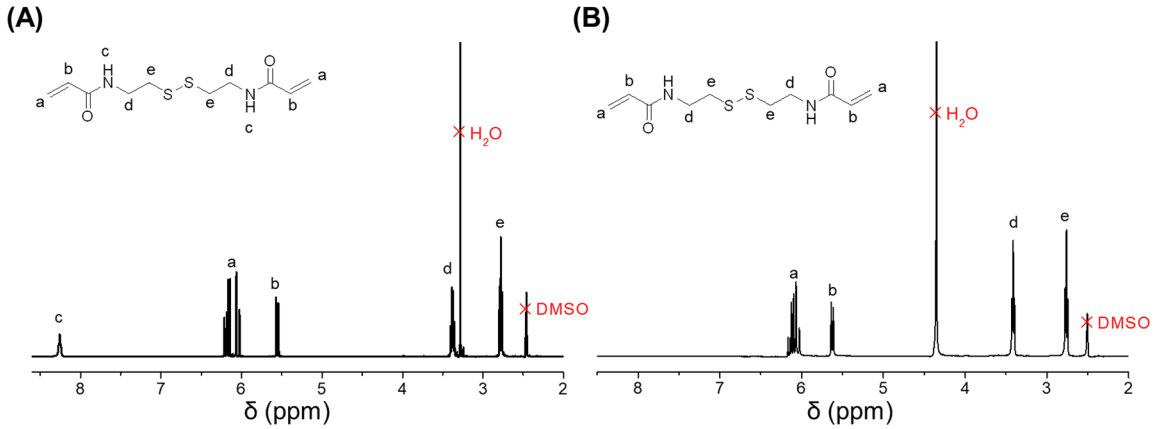

Fig. S2 ^{1}H NMR spectra of BAC monomer in (a) DMSO-d_6 and (b) D_2O/DMSO-d_6 = 1/1 (v/v).

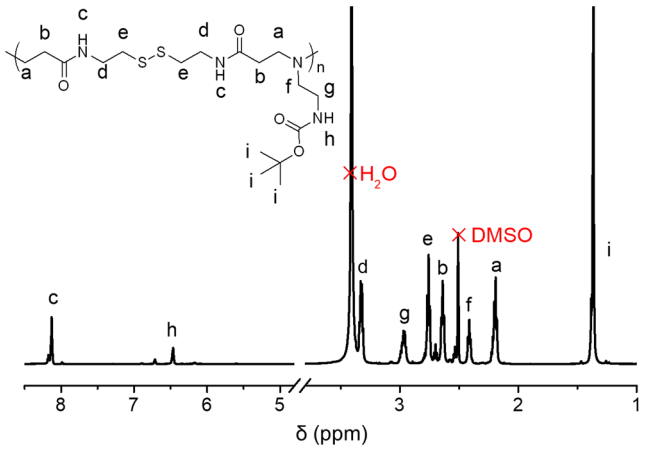

Fig. S3 ^{1}H NMR spectrum of polymer PBBE in DMSO-d_6.

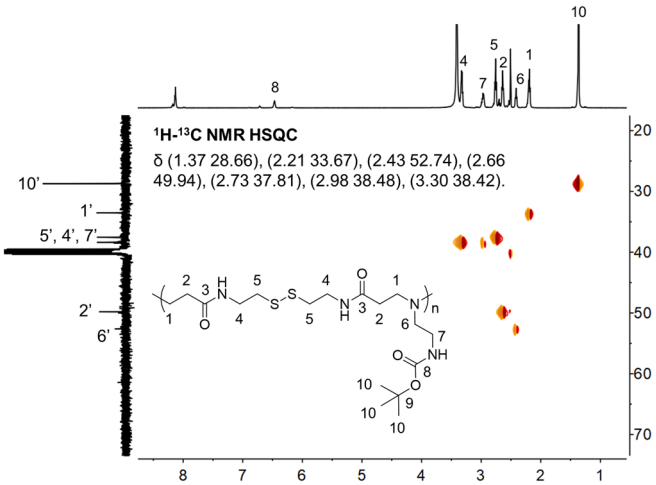

Fig. S4 ^{1}H-^{13}C HSQC spectrum of polymer PBBE in DMSO-d_6, to confirm the assignments in **Fig. S3**.

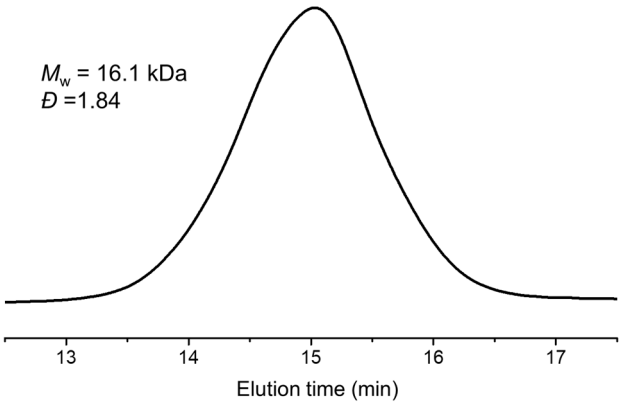

Fig. S5 SEC trace of PBBE in DMF (60 °C, 0.1 wt% LiBr) after three days of dialysis.

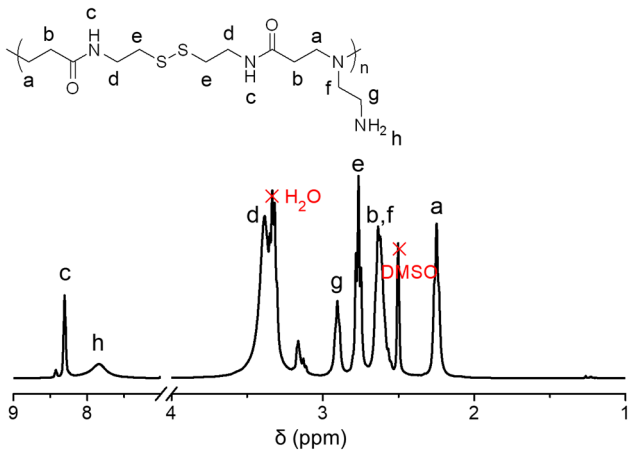

Fig. S6 ^{1}H NMR spectrum of polymer PBE in DMSO-d_6.

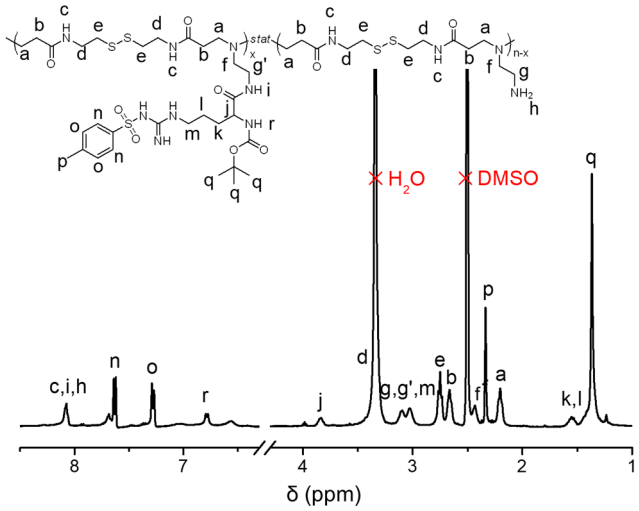

Fig. S7 ^{1}H NMR spectrum of polymer PBBR in DMSO-d_6.

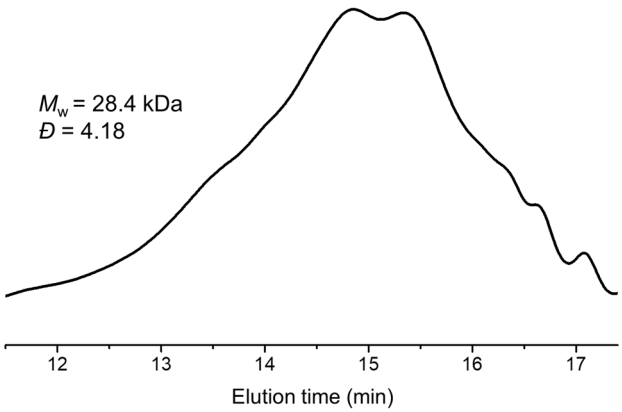

Fig. S8 SEC trace of PBBR in DMF (60 ºC, 0.1% wt LiBr).

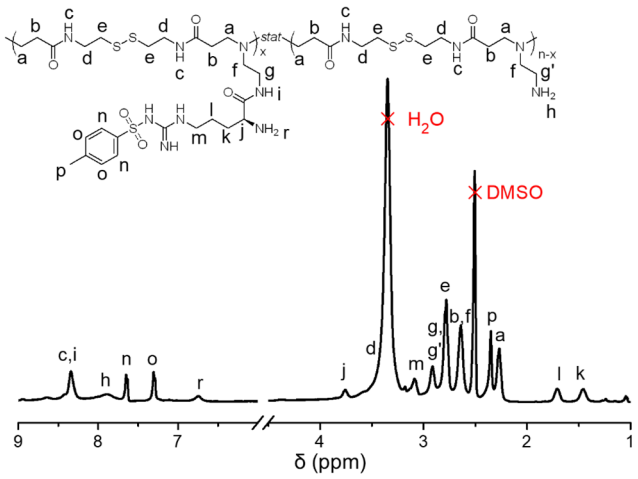

Fig. S9 ^{1}H NMR spectrum of PBR in DMSO-d_6.

Table S1. Integral areas and calculation of grafting density (G) of N^{ω}-*p*-tosyl-L-arginine

Polymer	$A_{(a+p)}/A_{(o+n)}$	G
PBR-1	10.25	11%
PBR-2	3.52	36%
PBR-3	2.37	62%
PBR-4	1.81	95%

In **Table S1**, $A_{(o+n)}$, $A_{(a+p)}$ are the integral areas of peaks o+n (phenyl group of N^{ω}-*p*-tosyl-L-arginine, 4x H) and a+p (a: methylene group near the tertiary amine of polymer main chain, 4n H, p: phenyl group of N^{ω}-*p*-tosyl-L-arginine, 3x H), respectively, in **Fig. S9**. Then the values of grafting density (G) of *p*-toluylsulfonyl arginine are obtained according to the following equations:

$$A_{(o+n)} = 4x$$

$$A_{(a+p)} = 3x + 4n$$

$$\mathrm{G} = 100\% \times \frac{x}{n} = 100\% \times \frac{4A_{(o+n)}}{4A_{(a+p)} - 3A_{(o+n)}} = 100\% \times \frac{4}{4 \times \frac{A_{(a+p)}}{A_{(o+n)}} - 3}$$

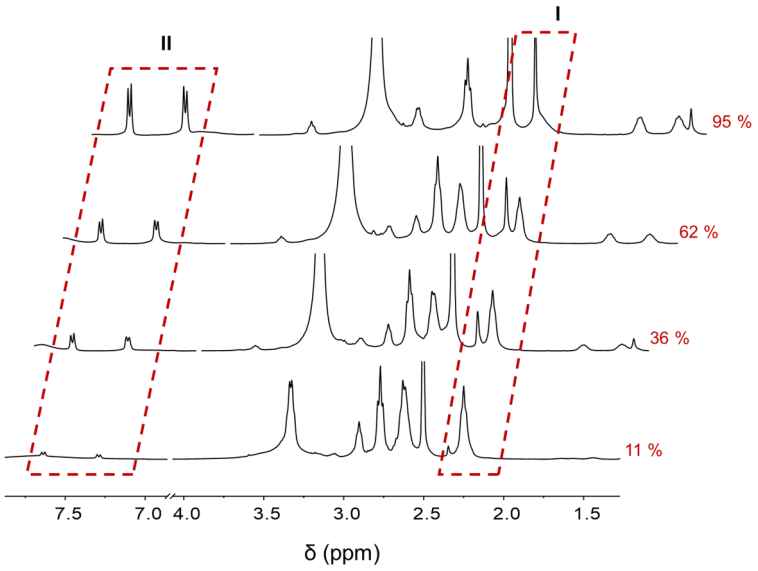

Fig. S10 Changes in the ^{1}H NMR spectra of different PBRs with different grafting density in DMSO-d_6. Region I and region II represent the $A_{(a+p)}$ and $A_{(o+n)}$, respectively.

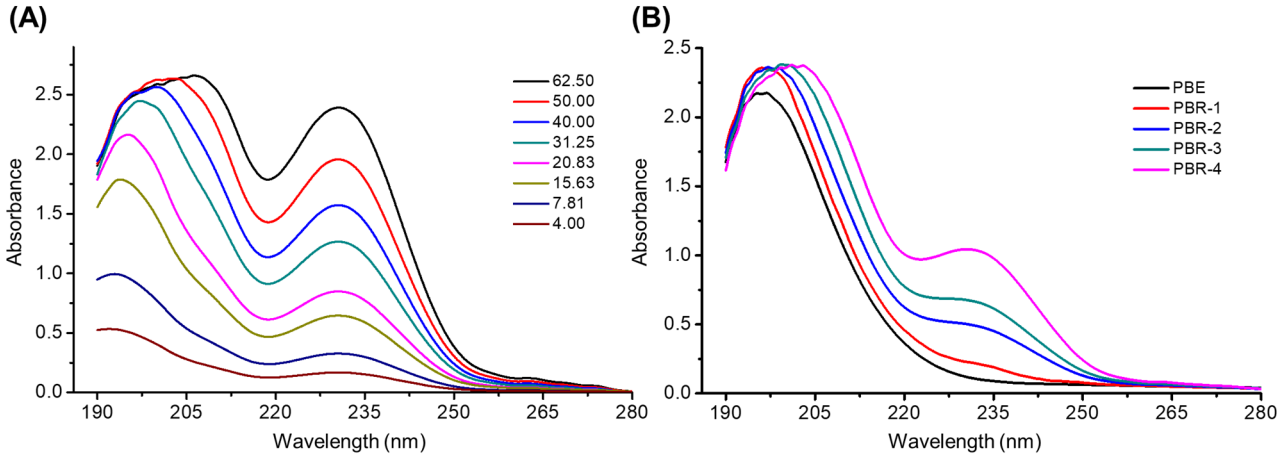

Fig. S11 (A) UV-Vis spectra of N^{ω}-*p*-tosyl-L-arginine at various concentrations (μg mL^{-1}) in water. (B) UV-Vis spectra of PBE and different PBR polymers (50 μg mL^{-1}) in water. The absorption peak around 230 nm originates from the N^{ω}-*p*-tosyl-L-arginine, and the increase in absorbance of it indicates the increasing grafting density of PBR.

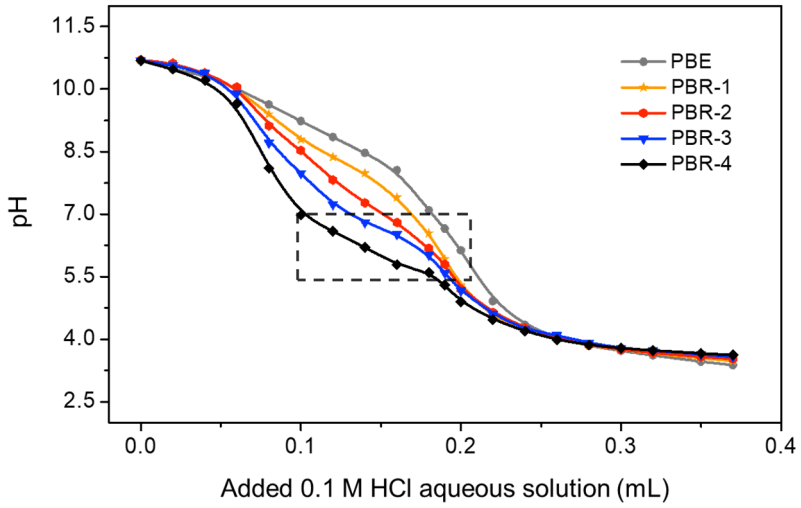

Fig. S12 Titration curve of PBE and different PBR polymers (0.5 mg mL^{-1}).

Table S2. Variable settings during optimization of PBE/siRNA complexation procedure (mean ± SD, n = 3)

No.	Weight ratio[a]	Concentration ratio[b]	N/P value	pH of polymer buffer solution	Hydrodynamic diameter (nm)	PDI	Zeta potential (mV)
1	1	4	2	7.4	551.5 ± 26.4	0.288	-19.1 ± 1.2
2	5	20	10	7.4	415.0 ± 14.2	0.129	-20.9±0.4
3	10	40	20	7.4	396.4 ± 16.0	0.257	-5.6 ± 1.1
4	15	60	30	7.4	367.5 ± 11.3	0.172	9.1 ± 0.6
5	20	80	39	7.4	313.9 ± 6.7	0.137	12.6 ± 0.3
6	25	100	49	7.4	287.2 ± 7.3	0.193	13.6 ± 0.5
7	15	60	30	6.4	212.2 ± 18.0	0.278	17.4 ± 0.5
8	15	62	30	6.4	228.4 ± 7.5	0.207	21.2 ± 0.3
9	15	76	30	6.4	191.4 ± 15.8	0.339	28.7 ± 0.7
10	15	96	30	6.4	179.7 ± 16.3	0.404	22.5 ± 1.4
11	15	127	30	6.4	146.0 ± 1.8	0.211	21.6 ± 2.2
12	15	181	30	6.4	163.2 ± 11.3	0.249	22.8 ± 1.6
13	15	304	30	6.4	211.4 ± 3.4	0.363	26.0 ± 0.8

[a]PBE/siRNA (μg $μg^{-1}$).

[b]Concentration of PBE in HEPES buffer/concentration of siRNA in HEPES buffer (μg $μL^{-1}$/μg $μL^{-1}$).

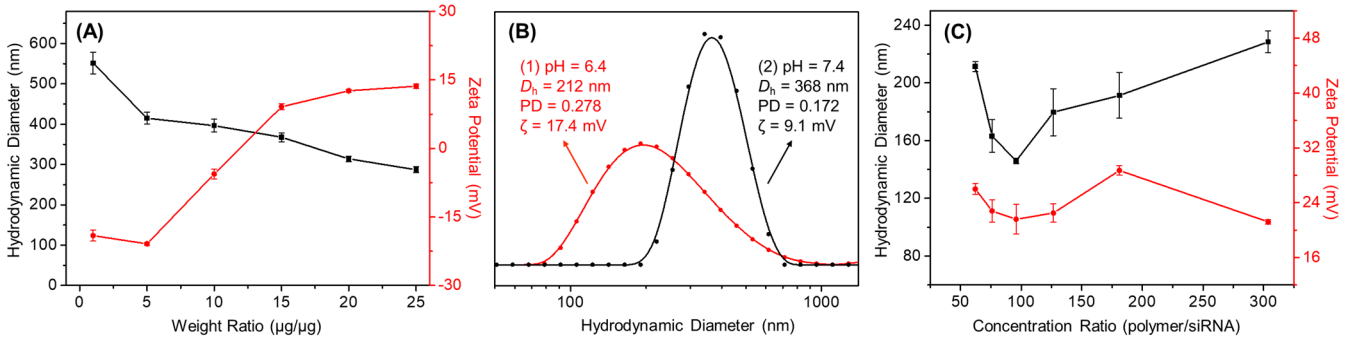

Fig. S13 DLS study and Zeta potential of different PBE/siRNA nanocomplexes in HEPES buffer in optimizing procedure. (A) PBE/siRNA nanocomplexes prepared with different weight ratio of PBE/siRNA (No.1-6 in **Table S2**). (B) PBE/siRNA nanocomplexes prepared at different pH values of PBE buffer solution (No.4 and No.7 in **Table S2**). (C) PBE/siRNA nanocomplexes prepared with different concentration ratios of PBE and siRNA buffer solution (No.8-13 in **Table S2**). The concentration ratio is expressed as the ratio of initial concentrationof PBE (μg mL^{-1}) to the initial concentration of siRNA (μg mL^{-1}) in their respective HEPES buffer at the beginning of the titration.

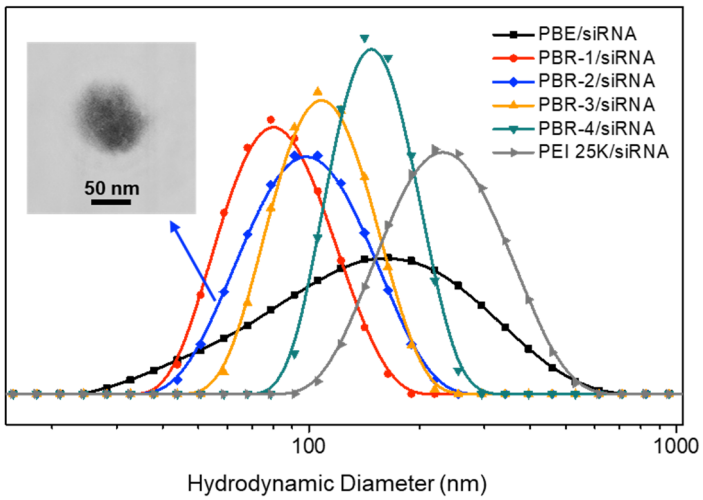

Fig. S14 Size distribution of different nanocomplexes as determined by dynamic light scattering (DLS) and typical transmission electron microscopy (TEM) image of PBR-2/siRNA nanocomplexes.

Table S3. Corresponding data of DLS studies of PBE/siRNA and different PBR/siRNA nanocomplexes in **Fig. S14** (mean ± SD, n = 3)

Formulation	RNA conc. (nM)	Polymer conc. (μg mL^{-1})	Weight ratio	Hydrodynamic diameter (nm)	PDI	Zeta potential (mV)
PBE/siRNA	1000	200	15	117.0 ± 2.4	0.268	21.3 ± 1.6
PBR-1/siRNA	1000	200	15	85.0 ± 1.8	0.179	24.9 ± 0.3
PBR-2/siRNA	1000	200	15	93.3 ± 1.0	0.081	27.4 ± 0.8
PBR-3/siRNA	1000	200	15	103.5 ± 2.3	0.044	29.7 ± 0.3
PBR-4/siRNA	1000	200	15	155.4 ± 3.7	0.041	34.7 ± 1.0
PEI 25K/siRNA	1000	40	3	217. 7± 2.5	0.101	28.4 ± 0.8

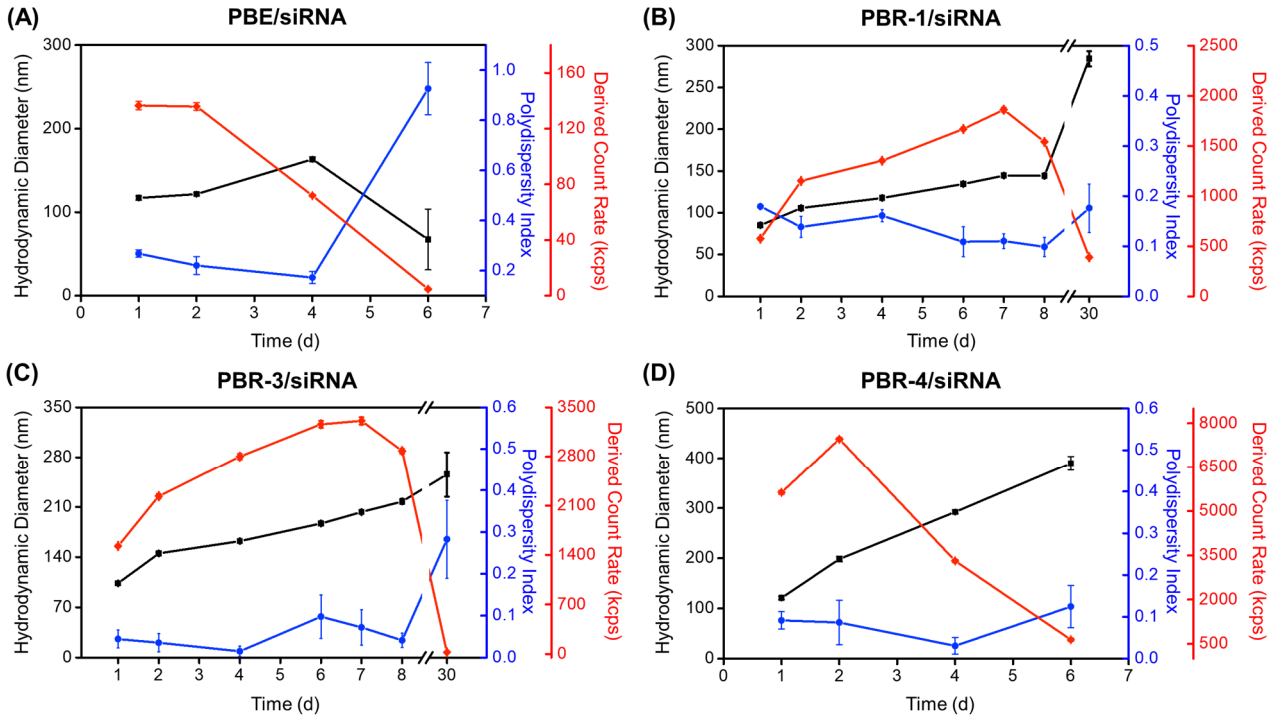

Fig. S15 DLS analysis of PBE/siRNA and different PBR/siRNA nanocomplexes over time in HEPES buffer (20 mM HEPES, 5.0 wt% glucose in water, pH 7.4, 4 ºC storage).

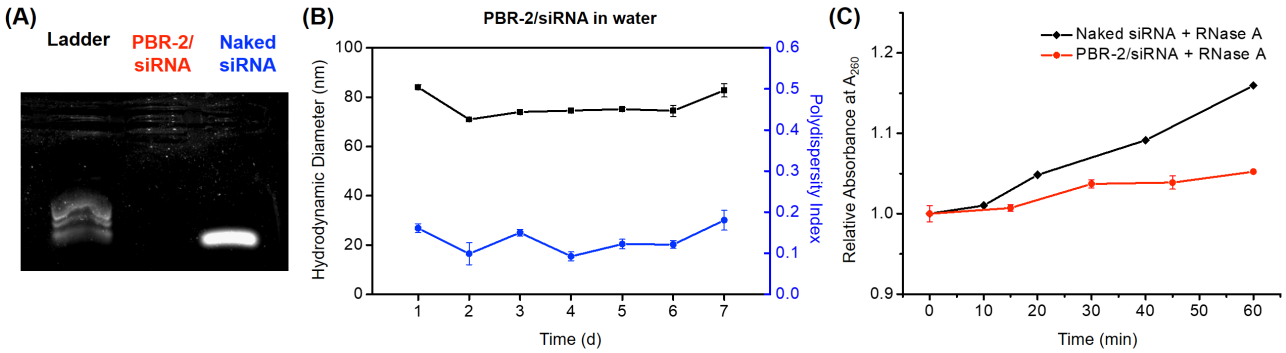

Fig. S16 (A) Agarose gel retardation analysis of the naked siRNA and PBR-2/siRNA nanocomplexes. (B) DLS analysis of PBR-2/siRNA (100 nM siRNA) over time in diluted aqueous solution (4 ºC storage). (C) Changes of relative UV-Vis absorbance at 260 nm of naked siRNA and PBR-2/siRNA nanocomplexes over time in the presence of 1.0 μg mL^{-1} RNase A in HEPES buffer at 25 ºC, pH 7.4. The relative absorbance at 260 nm of naked siRNA increased obviously faster than that of PBR-2/siRNA nanocomplexes.

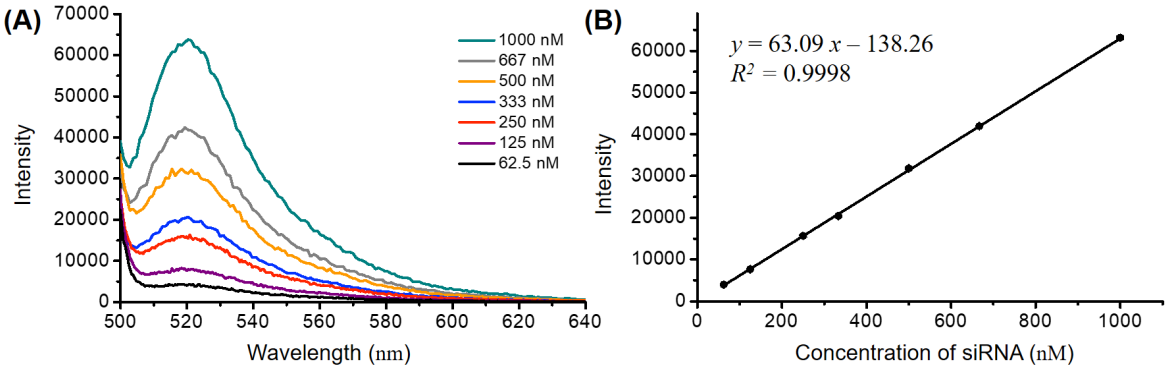

Fig. S17 (A) The fluorescence spectra of FAM-siRNA at different concentrations and (B) the calibration curve of FAM-siRNA in HEPES buffer (λ_{ex} = 492 nm).

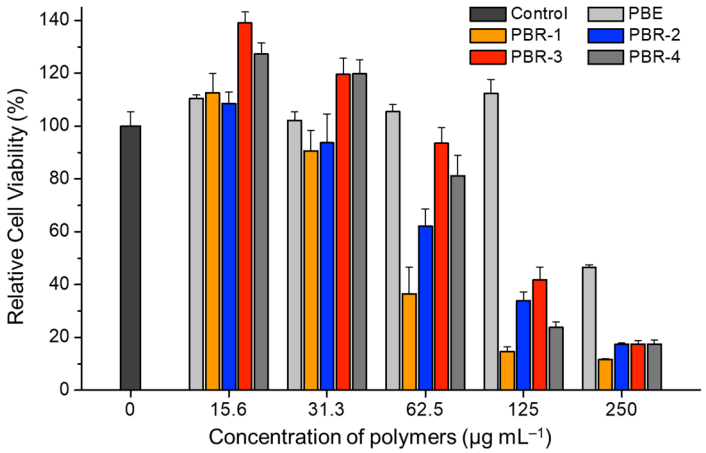

Fig. S18 Relative cell viability of L02 cells after incubation with increasing concentrations of different polymers for 24 h. The cytotoxicity is negligible when the concentration of polymers is less than 31.3 μg mL^{-1}.

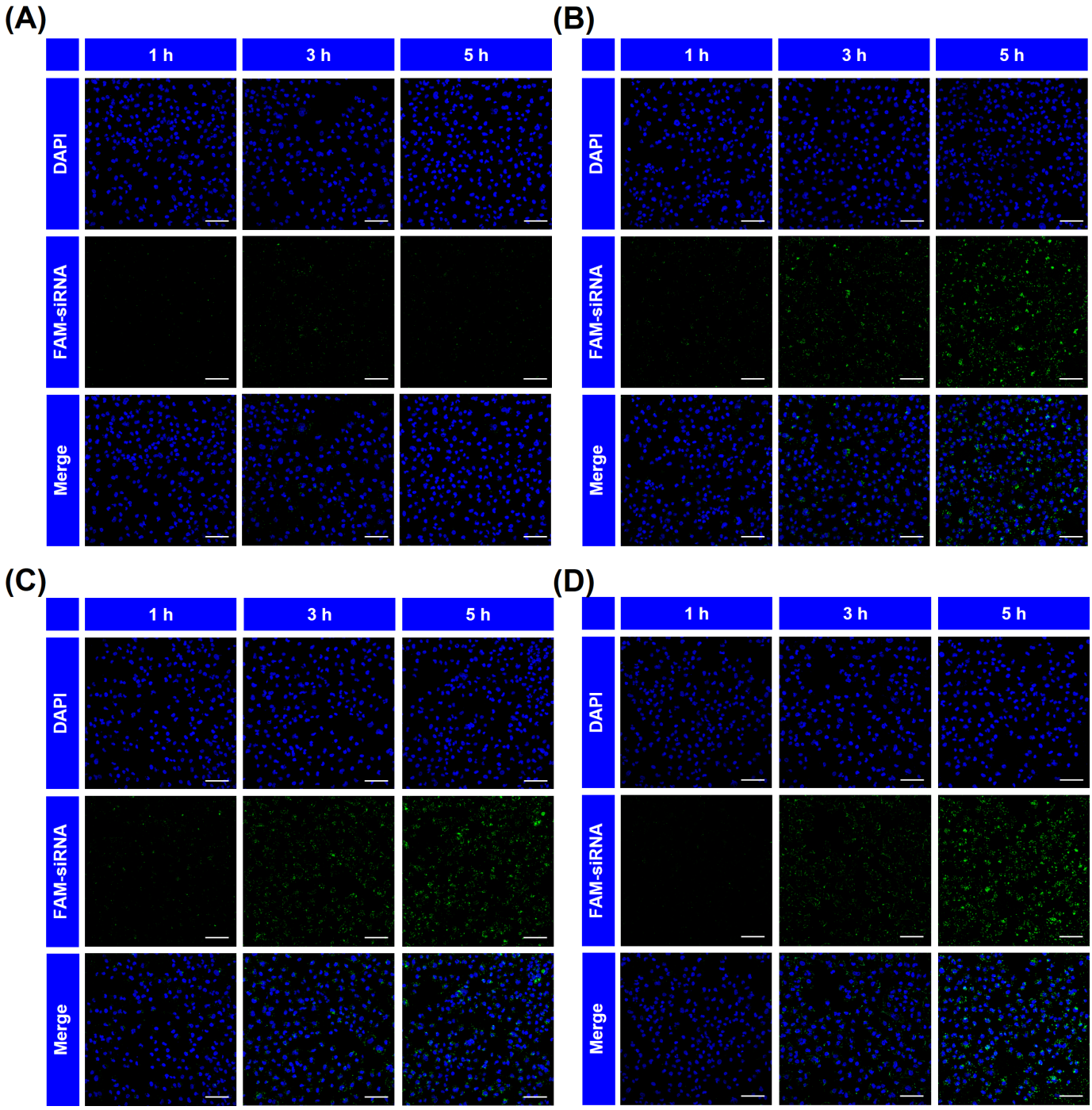

Fig. S19 Visualization of the degree of cellular uptake of (A) PBE/FAM-siRNA, (B) PBR-1/FAM-siRNA, (C) PBR-3/FAM-siRNA and (D) PBR-4/FAM-siRNA nanocomplexes in PANC-1 cells. Representative CLSM images were taken after different co-incubation time of 1, 3, and 5 h. Green channel: FAM labeled siRNA. Blue channel: the nuclei of PANC-1 cells stained by DAPI. Scale bar: 100 μm.

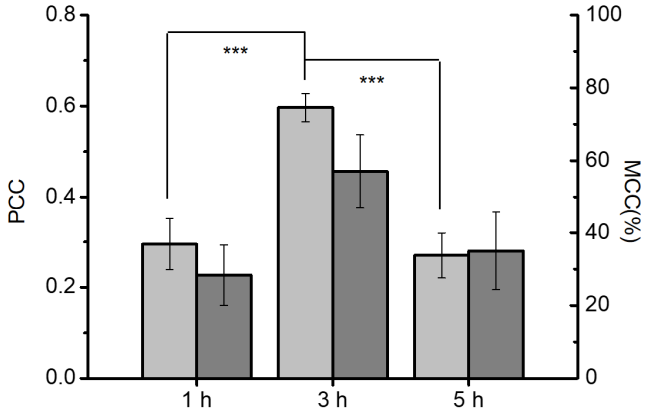

Fig. S20 PANC-1 cells were incubated with PBR-2/FAM-siRNA nanocomplexes for 1, 3 and 5 h. PCC (Pearson's correlation coefficient) and MCC (Manders' colocalization coefficients) were calculated from the CLSM images for colocalization analyses of PBR-2/FAM-siRNA nanocomplexs (green) and lysosome tracker (red) using ImageJ software. Data are presented as mean ± SD (n = 3). One-way analysis of variance (ANOVA) was performed to evaluate the significance of the experimental data. A value of 0.05 was selected as the significance level, and the data were indicated with (***) for $p < 0.001$.

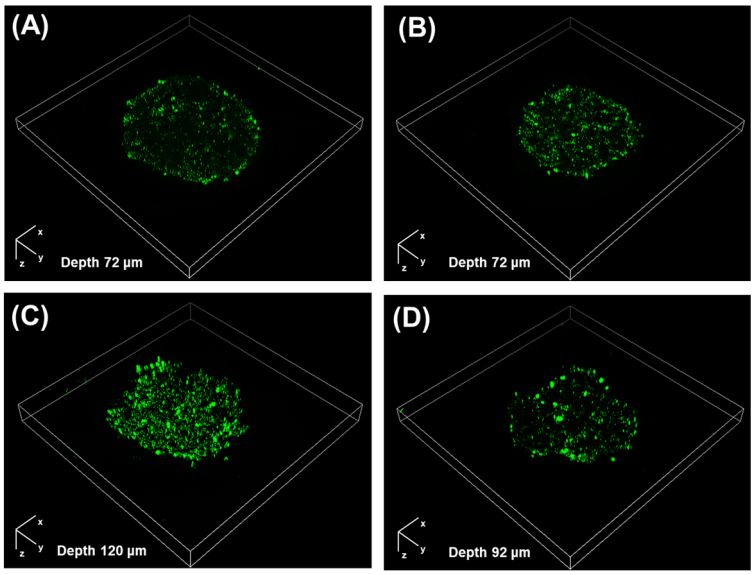

Fig. S21 CLSM 3D images of *in vitro* penetration of FAM labeled PBR-2/siRNA nanocomplexes in PANC-1 multicellular spheroids (MCSs). The MCSs were incubated with PBR-2/siRNA nanocomplexes (100 nM siRNA equivalent) for (A) 3, (B) 6, (C) 9 and (D) 18 h, then taken out, washed with PBS and observed by CLSM Z-stack scanning.

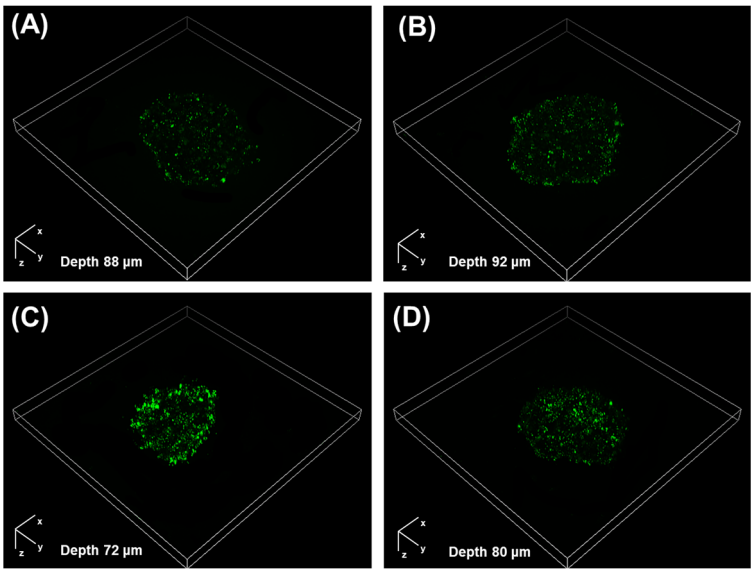

Fig. S22 CLSM 3D images of *in vitro* penetration of FAM labeled PBE/siRNA nanocomplexes in PANC-1 multicellular spheroids (MCSs). The MCSs were incubated with PBE/siRNA nanocomplexes (100 nM siRNA equivalent) for (A) 3, (B) 6, (C) 9 and (D) 18 h, then taken out, washed with PBS and observed by CLSM Z-stack scanning.

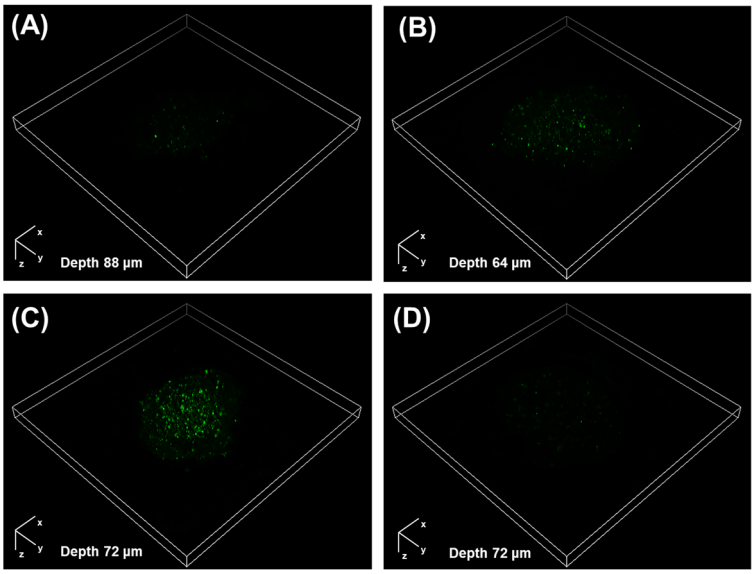

Fig. S23 CLSM 3D images of *in vitro* penetration of FAM labeled PEI 25K/siRNA nanocomplexes in PANC-1 multicellular spheroids (MCSs). The MCSs were incubated with PEI 25K/siRNA nanocomplexes (100 nM siRNA equivalent) for (A) 3, (B) 6, (C) 9 and (D) 18 h, then taken out, washed with PBS and observed by CLSM Z-stack scanning.